Arterial Extracellular Matrix: A Mechanobiological Study of the Contributions and Interactions of Elastin and Collagen

Ming-Jay Chow,[†] Raphaël Turcotte,[‡§] Charles P. Lin,[§] and Yanhang Zhang[†‡]*

[†]Department of Mechanical Engineering and [‡]Department of Biomedical Engineering, Boston University, Boston, Massachusetts; and [§]Center for Systems Biology, Advanced Microscopy Program, Wellman Center for Photomedicine, Massachusetts General Hospital, Harvard Medical School, Boston, Massachusetts

Appendix:

FFT Analysis:

The full description of the processing used by Directionality is found in detail online (http://fiji.sc/Directionality) and in the work by Liu [1]. Briefly, the program divides an image into smaller square sections, in which the preferred orientation was provided through Fourier transform calculations. To aid viewing, the orientation of the fibers is displayed with colors and the histogram of the orientations is also generated as seen in schematic process of Figure A1.

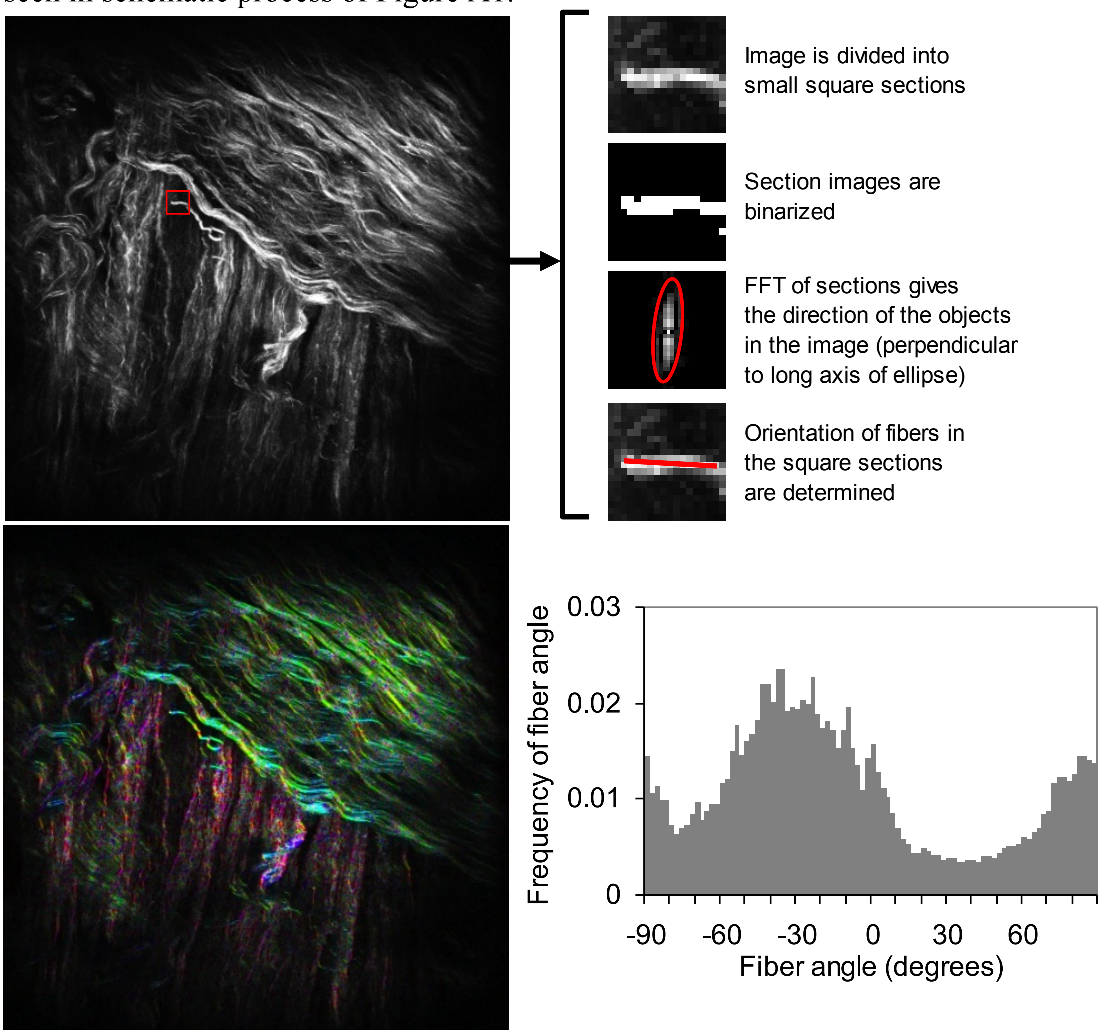

Figure A1: Schematic of processing method of Directionality plugin. An image (top left) is divided into small squares and the orientation of each region is calculated with a FFT process. The orientations throughout the image are presented either based on coloring of the original image (bottom left) or with a distribution of fiber angles (bottom right).

While the FFT method is well established for determining the main fiber orientation, the results should be interpreted carefully as the method is sensitive to other structural changes as well. Figure A2 provides an examination of the effect of waviness on the FFT analysis. With straightened fibers, the FFT analysis generates a histogram with a high and narrow peak, as expected (Figure A2, top row). If the fibers are wavy, the FFT analysis has a wider distribution of fiber angles around the main direction (Figure A2, middle row). It is important to note that, in this case, the main fiber direction is correctly reported by the FFT and there is no bias towards any particular orientation. As an example, the image from the middle row of Figure A2 was rotated by 90° and the resulting distribution is exactly the same but is offset by 90° (Figure A2, bottom row). In an example of extremely wavy fibers (Figure A3), various regions along a single fiber resulted in orientations between -90° and 0° although the main fiber angle is -38°. The undulation from largely wavy fibers can mask the real fiber orientation and results in a wide distribution with no identifiable peak in the main fiber direction.

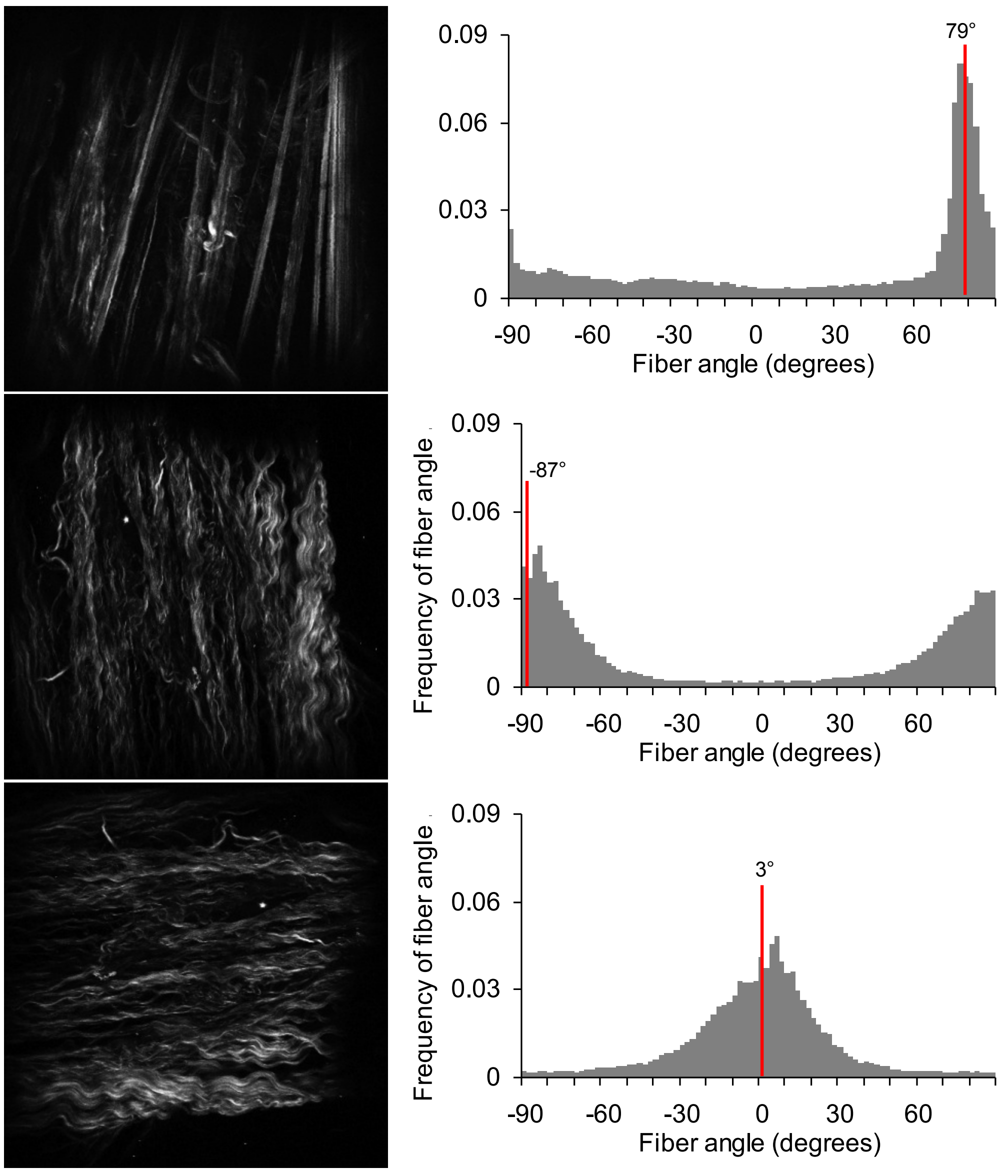

Figure A2: Effect of fiber waviness on FFT analysis with Directionality plug-in. Top row: relatively straight fibers result in a histogram with a high and narrow peak; middle row: wavy fibers with main fiber direction properly determined, but with increased width of the distribution; bottom row: the image from the middle row was rotated by 90° and the resulting distribution is exactly the same but is offset by 90° showing that there is no bias towards any particular orientation. Images are 360×360μm

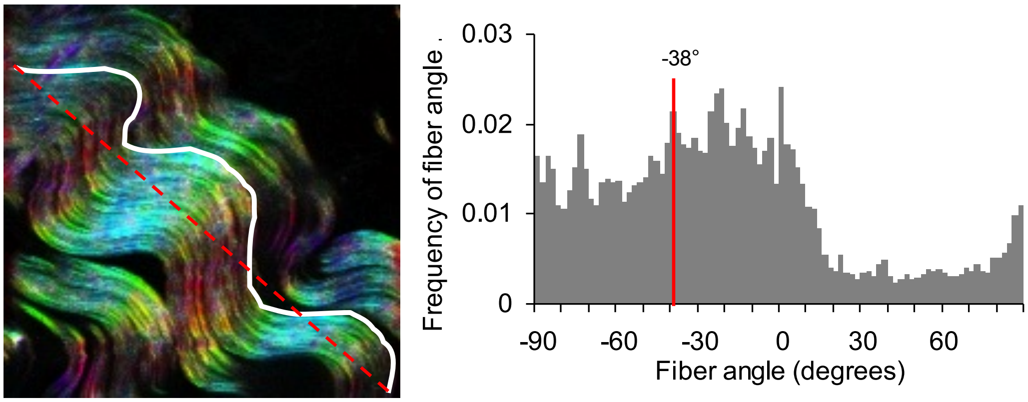

Figure A3: Effect of fiber waviness on FFT analysis with Directionality plug-in showing that largely wavy fibers can mask the real fiber orientation and results in a wide distribution with no identifiable peak in the main fiber direction. Image is 110×110μm.

Another structural change that can be captured by the FFT results is the change in fiber alignment. Synthetic images were generated with straight lines oriented at -45° with Matlab. As the standard deviation of the lines around the -45° angle was increased from 1, 5, to 10°, the resulting FFT distribution had a lower max peak and wider distribution, as expected (Figure A4). This trend is very similar to what occurs due to increased waviness in the fibers as shown in Figure A3 and it is not possible to identify to what degree the waviness and change in alignment in the real images contributes to the difference in FFT results.

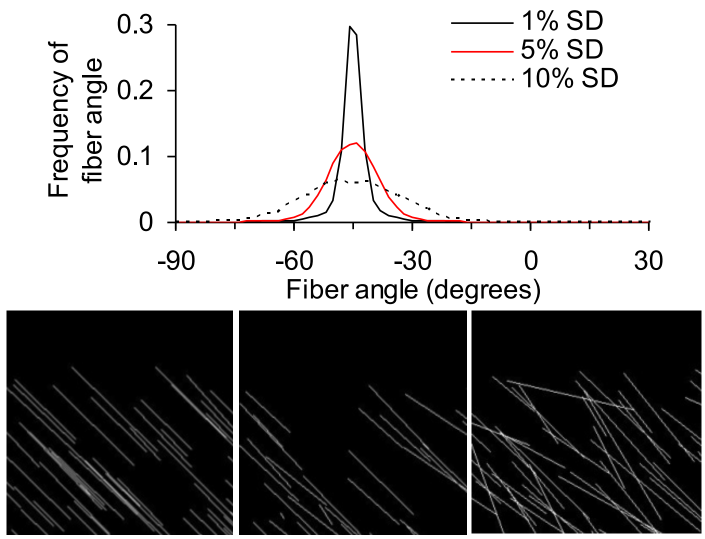

Figure A4: Effect of fiber alignment on FFT analysis with Directionality plug-in. The standard deviation around the main fiber angle (-45°) was increased to 1°, 5°, and 10° resulting in a wider distribution.

The experimental protocols included using constant laser powers and consistent image acquisition settings in order to minimize the variation in image intensity and noise. To verify the image analysis methods, experimental images were modified with ImageJ protocols to examine the effects of noise and intensity. ImageJ was used to change the intensity of example adventitial collagen images from 0 to 100% of the original. Even with the change in intensity seen in Figure A5 (22-100% of original), there was no change in the fiber distributions as measured with Directionality. If the intensity was below 10% the FFT analysis did start to report more random/uniform fibers but all experimental images had intensities necessary to obtain a repeatable result. The average intensities of medial collagen and elastin images did not vary with stretch.

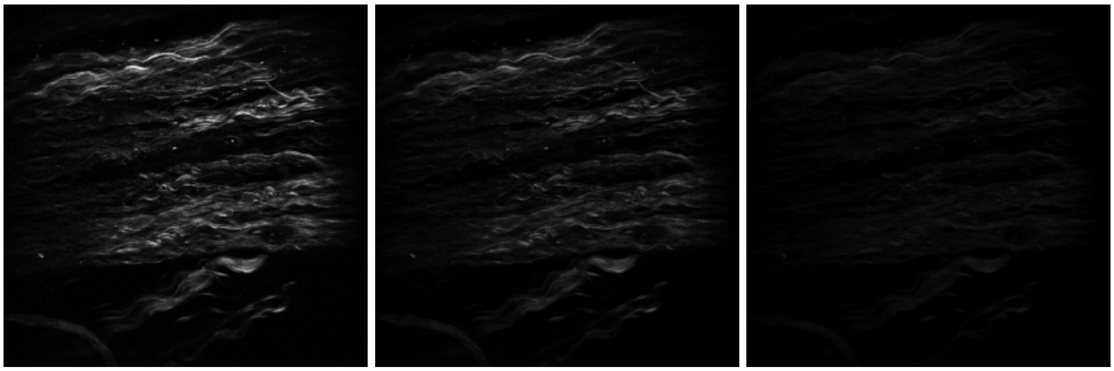

Figure A5: Example adventitial collagen images with intensity modified with ImageJ. The intensities of the images relative to the original are at 100% (left, aka original image), then 61% (middle), and 22% (right) and had no effect on fiber orientation distributions. Images are 360×360μm.

To assess the effect of noise, ImageJ was used to add noise with 6% and 12% of standard deviation, with the later corresponding to a greater amount of noise than in any of the experimental images. Figure A6 shows the same adventitial collagen after being processed to have more noise. This resulted in no change of the major peaks in the FFT analysis but did decrease the peak height as more random fiber orientations were detected. Note that because the FFT output from Directionality is normalized, an image of pure noise (random) gives a flat distribution with a height of 0.011 because of our choice to use 90 bins (1/90 = 0.011).

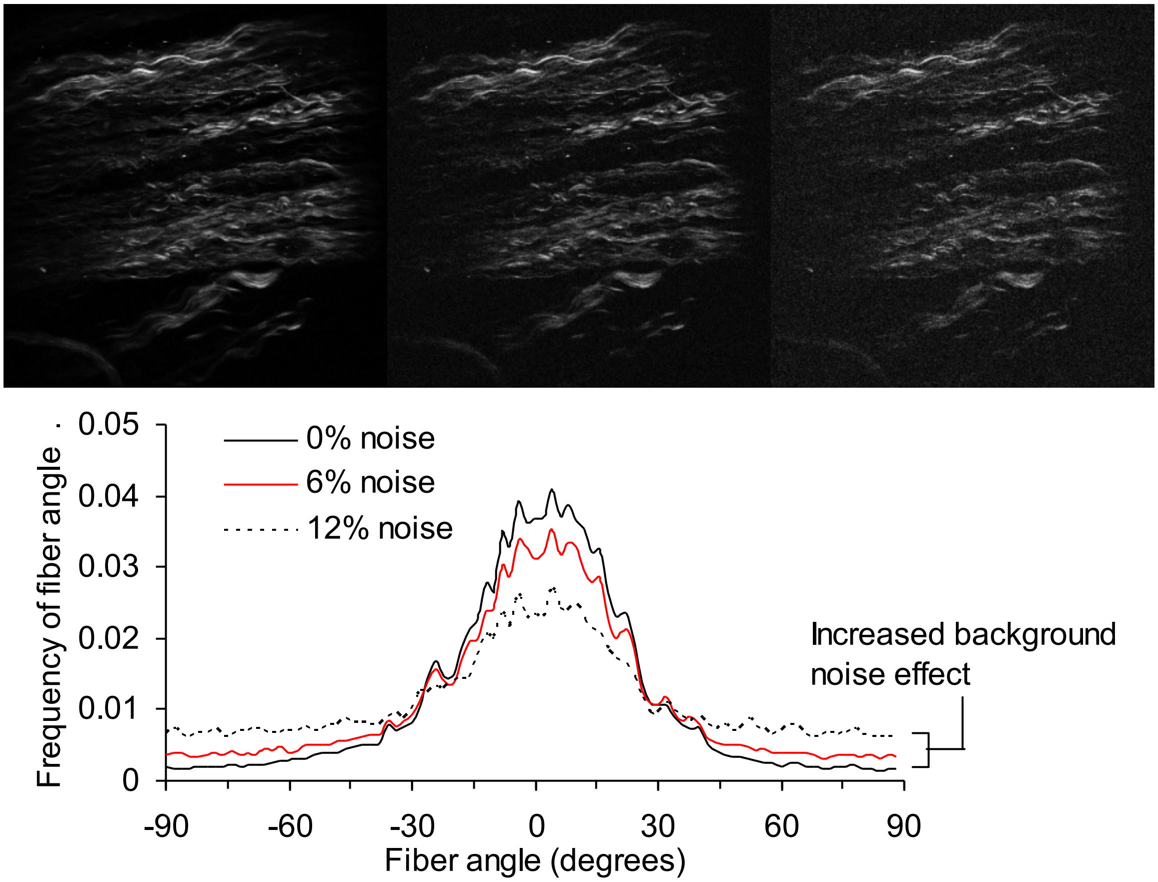

Figure A6: Example adventitial collagen image with random noise modified with ImageJ. The noise level in unchanged (left), then increased by 6% (middle), and 12% (right). The resulting Directionality results show the main fiber orientation is still successfully detected but the peak is lower as the background noise level increases. Images are 360×360μm.

Throughout our validation studies that included modifying experimental images as well as synthetic images generated through Matlab, the FFT analysis was capable of accurately determining fiber direction. Fiber waviness, fiber splay, and image noise were shown to have an effect on the FFT results but not to the extent that the main fiber direction could not be determined. Extreme fiber waviness was the only condition that was tested that had the potential to mask the true fiber direction.

Fractal analysis:

To determine fractal number in Eq. 2, a direct relationship between box size and box number is not possible for real images so a plot of $\log(N_r)$ vs $\log(r)$ can be best fitted and the slope will be an approximate value of D (Figure A7). The fractal number for all 2D images varies between 1 (for a straight line) and 2 (for a square).

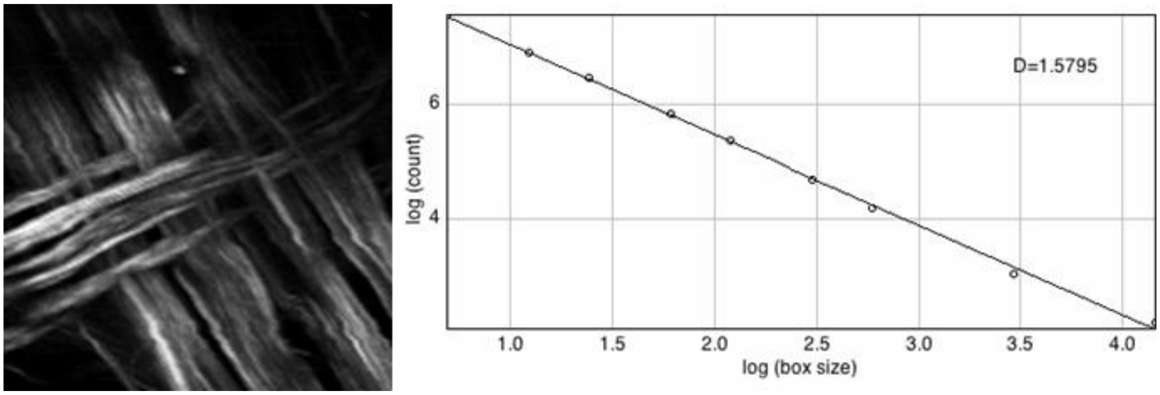

Figure A7: Example of the fractal analysis of a sample image. A SHG image (left, 110x110µm) of adventitial collagen yields the plot of log(Nr) vs. log(r) and a fractal number of 1.5795 (right).

Test images were generated with a custom Matlab (Mathworks, Natick, MA, USA) code to examine how the fractal number would change in response to specific differences in images (Figure A8). The first series of generated images (top row) consisted of a normal distribution of straight lines where the standard deviation of the distribution was decreased so the lines became more aligned. The second set of test images (middle row) consisted of sine wave functions of the form $y = \sin(2\pi(f))$ with decreasing frequencies so there was less waviness in the lines. These synthetic images examine two possible ways in which fibers can be engaged to support mechanical loading. The loss of "crimping" in the sine waves coincide with larger differences in the fractal number as further confirmation of the usefulness of the fractal number to detect changes in waviness. However, the increasingly aligned lines in the top row of Figure A8 also corresponded with an increase in fractal number. This indicates that the fractal method is sensitive to not only changes in fiber waviness but other mechanisms of fiber engagement as well.

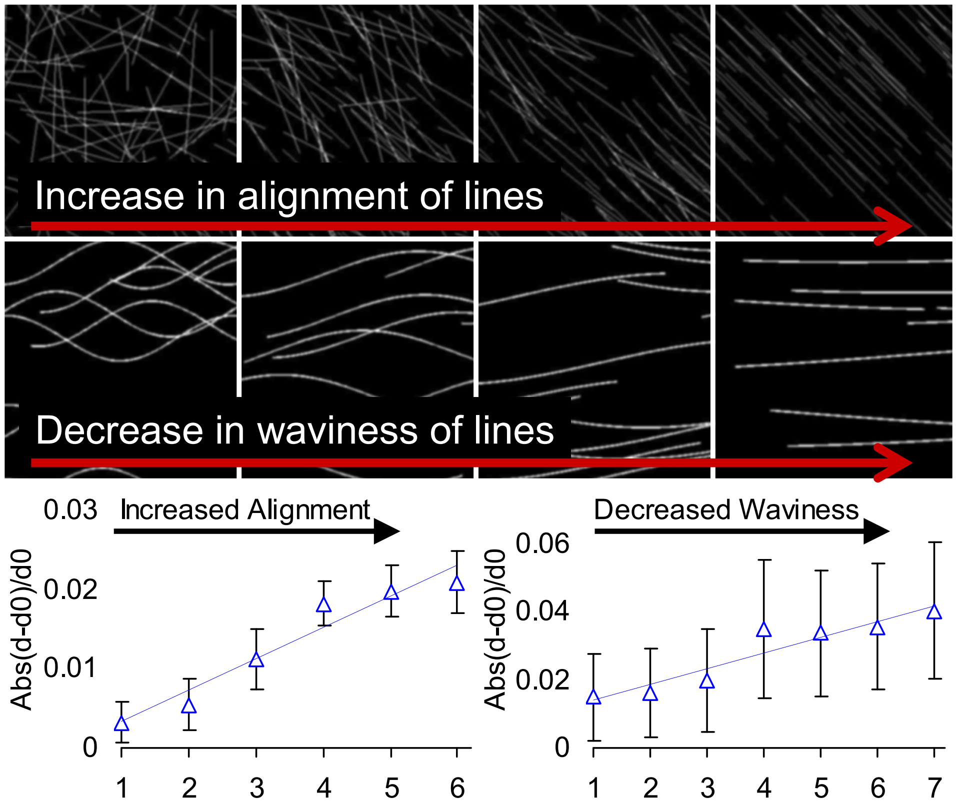

Figure A8: Test images used to determine the effect of alignment (top row) and waviness (middle row) on fractal analysis. Both test image groups showed increasing difference in fractal number (bottom row).

It was noted that the adventitial collagen images contained the most variability in image intensity and that the intensity generally increased with stretch. This could be due to a combination of factors such as molecular changes and aggregation of the fibers leading to a stronger SHG signal. The effects of intensity on the fractal analysis was examined by normalizing the mean intensity of adventitial collagen images at deformed state to the initial image intensity at 0% strain, so that all images have the same average intensity. As a result of the changing the intensity, fractal analysis on both sets of images reveals no qualitative change in the descriptive of fiber engagement (Figure A9, left). We decided not to normalize images to have the same intensity because this could remove some structural change information. The effect of noise on the fractal method was investigated in a similar manner as performed to verify the FFT analysis with 6% and 12% of standard deviation added (Figure A9, right). The absolute and normalized differences in fractal number is only minimally changed and it was determined that the amount of noise in our images was below the threshold necessary to affect the results.

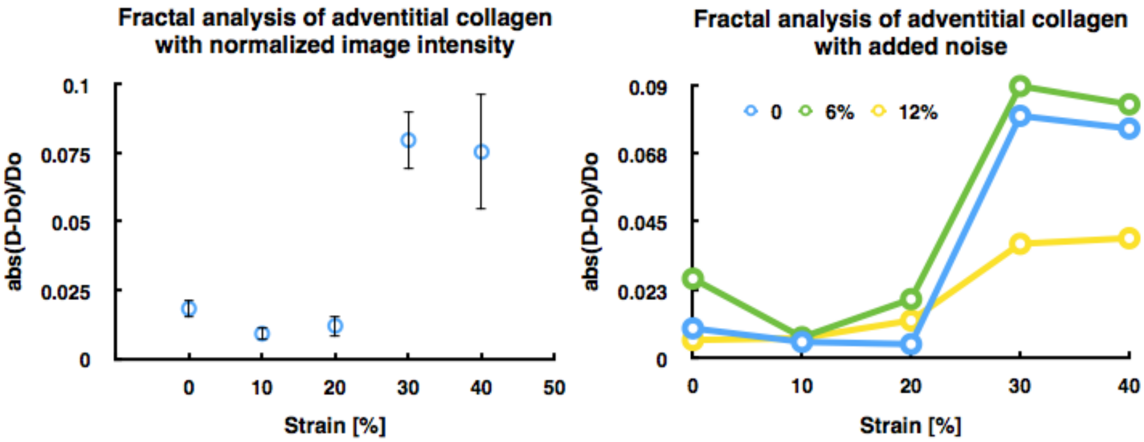

Figure A9: Effect of image intensity and image noise on the fractal analysis. Fractal analysis of adventitial collagen on normalized images (left) and images with added noise (right) shows that the trends observed with the fractal analysis are not affected by changes in intensity or noise at the levels present in our data set.

Reference:

1. Liu, Q.Z. 1991. Scale space approach to directional analysis of images. Appl. Opt. 30(11): 1369-1373.